



Efficient enzymatic hydrolysis of cellulose treated by mixed ionic liquids

Qiang Li^{1,2} · Gengsheng Ji¹ · Yongle Chen² · Yun Xu³ · Jingyu Shen² · Youting Wu²

Received: 4 November 2019 / Accepted: 24 April 2020 / Published online: 9 May 2020
© Institute of Chemistry, Slovak Academy of Sciences 2020

Abstract

In recent years, ionic liquids (ILs) have been confirmed to be efficient and green solvent for treatment of cellulosic biomass toward subsequent bioprocess. However, few attempts have been made to use mixed ILs as solvent to treat cellulose. In order to expand the scope of IL and mixed ILs used for cellulose treatment, we developed mixed ionic liquids as reagent to treat cellulose. Subsequently, the treated cellulose and treatment process were assessed by measuring the indexes of cellulose in and after treatment process. As a result, mixed ILs combination 1-methyl-3-methylimidazolium dimethylphosphate ([DMIM][DMP]) and 1-ethyl-3-ethylimidazolium bisulfate ([EMIM][HSO₄]) were selected as a candidate reagent for cellulose treatment. Unlike some other studies, not only outermost surface of cellulose was changed, but structure of cellulose was destroyed and converted into 3–6 μm particles, resulting in almost complete enzymatic hydrolysis of treated cellulose within 12 h. In addition, the initial rate of enzymatic hydrolysis of cellulose treated by candidate mixed ILs was 56.3 times that of water-treated cellulose (control). It was demonstrated that intact structure of cellulose was destroyed by mixed ionic liquids treatment and resulted in a new framework that greatly improved enzymatic hydrolysis, which opened a new way for efficient enzyme conversion of cellulosic biomass.

Keywords Mixed ionic liquids · Cellulose · Structure conversion · Enzymatic hydrolysis

Abbreviations

FT-IR Fourier transform infrared spectroscopy
SEM Scanning electron microscope

Introduction

Cellulose is the widely available and renewable biomass on earth used in numerous applications (Houfani et al. 2020) such as consumables, paper products, energy crops and biofuels. Cellulose is a purified form of subunits of

poly- α -cellobiose derived from cellulosic biomass (Liu et al. 2017) and has great industrial interest because of its use either in chemicals (Zhu et al. 2020), liquid fuels (Chen and Lee 2020), or other industrial applications (pharmacology, cosmetics and even ceramics) (Kim et al. 2020; Li et al. 2019; Ullah et al. 2016).

Enzymatic conversion of cellulose is one of the promising routes to sustainably produce fuels and other chemicals (Jang et al. 2020). However, cellulosic biomass hydrolysis in aqueous media suffers from slow reaction rates (Sievers et al. 2017) for there are water-insoluble crystalline substrates in the biopolymers. They are very hard to degrade or dissolve for the extensive network of inter- and intra-molecular hydrogen bonds and van der Waals interactions between cellulose fibrils (Lv et al. 2020). Therefore, homogeneous treatment of cellulose using solvents has generated interest for many years and is still subject to ongoing research (Tan et al. 2019). During the last decade, a new type of green solvent known as ionic liquid (IL) has been paid more attention because most of them have the virtues of excellent solvency, nonvolatility, low melting point and designability (Xu et al. 2020). Furthermore, ionic liquid has been confirmed to be efficient and green solvent for treatment of cellulosic

Electronic supplementary material The online version of this article (<https://doi.org/10.1007/s11696-020-01176-4>) contains supplementary material, which is available to authorized users.

✉ Gengsheng Ji
biojustq@126.com

¹ School of Biotechnology, Jiangsu University of Science and Technology, Zhenjiang 212018, China

² School of Chemistry and Chemical Engineering, Nanjing University, Nanjing 210093, China

³ China Pharmaceutical University, Nanjing 210009, China

biomass (Jiang et al. 2020), resulted in ionic liquid involved treatment and enzyme conversion of cellulose toward value-added products has been paid more attention (Haldar and Purkait 2020).

Measuring the crystallinity, degree of polymerization (DP) (Sirvio et al. 2020), thermogravimetry analyses (TGA) (Ratnasari et al. 2019), crystallinity index (CrI), scanning electron micrographs (SEM) (Shah and Ullah 2019) and X-ray diffraction (XRD) (Bernardo et al. 2019), viscosity indexes analysis of cellulose in and after the treatment process is essential in assessing its correlation with the resulting technical properties in and after ionic liquid treatment for subsequent enzymatic conversion. However, as far as we know, there is no work on mixed ionic liquids treatment of cellulose and few systematic works on monitoring the ionic liquid treatment process and link the process to subsequent enzymatic reaction using different properties analysis of cellulose.

In order to expand the scope of IL and mixed ILs used for cellulose treatment and illuminate the mechanism of following efficient enzymatic process via indexes analysis of cellulose in and after the treatment process, herein, we report basic work on the treatment of cellulose in mixed ionic liquids for efficient enzymatic conversion. Three classic kinds of ionic liquids: phosphate-type ILs, chloride-type IL and bisulfate-type ionic liquids, were synthesized. Composition of mixed ILs to treat cellulose was accessed according to the characters of mixed ILs. ILs bearing sulfonate anion could treat surface area of cellulose to form porous carbon (Huang et al. 2020); however, there is no work on this issue of bisulfate-type ionic liquids for cellulose pretreatment. Therefore, treatment of cellulose using selected mixed ILs was investigated. Subsequently, enzymatic saccharification of cellulose after IL treatment was investigated. The viscosity of ILs and cellulose/IL solution was measured to analyze the intrinsic characters of IL treatment process. In addition, treated cellulose was measured by FT-IR, SEM, TGA, XRD and DP analysis to reveal the mechanism of the following efficient enzymatic process.

Experimental

Materials and methods

Materials

The following chemicals and enzyme were purchased from Sigma-Aldrich (St. Louis, MO, USA): *N*-methylimidazole, *N*-ethylimidazole, trimethyl phosphate, triethyl phosphate, 1-chlorobutane, ethyl acetate, bromoethane, diethylamine and cellulose 101 [Sigmacell Cellulose, highly purified, fibers, particle size 50 μm]. Cellulase from *Aspergillus*

niger (E.C. #3.2.1.4, slightly brown powder, 0.5 units/mg solid; Bradford reagent test suggested a protein content of 31 wt%) was purchased from KangYuan Biotec. One unit will liberate 1.0 μmol of glucose from cellulose in 1 h at pH 5.0 at 37 $^{\circ}\text{C}$ for 2-h incubation. IL 1-methyl-3-methylimidazolium dimethylphosphate ([DMIM][DMP]), 1-ethyl-3-ethylimidazolium diethylphosphate ([EMIM][DEP]), 1-ethyl-3-ethylimidazolium bisulfate ([EMIM][HSO₄]), 1-butyl-3-methylimidazolium bisulfate ([BMIM][HSO₄]), 1-ethyl-3-methylimidazolium chloride ([EMIM]Cl) and 1-butyl-3-methylimidazolium chloride ([BMIM]Cl) were synthesized and purified in the following literature (Li et al. 2010; Nie et al. 2006). Water content in the ionic liquids was in the range of 0.20–0.55 wt%, which was measured by Karl Fischer analyzer (METTLER TOLEDO). All other chemicals were of analytical grade and purchased from Sinopharm Chemical Reagent Company (SCRC, China).

Treatment of cellulose

Mixed ionic liquids were prepared by mixing two kinds of ionic liquids in a certain proportion (1:1 ~ 10, w/w) for 10 min at room temperature and heated to treatment temperature before treatment. Samples of cellulosic biomass solution (3%, w/w%) were prepared by combining 0.09 g of cellulose with 3.0 g IL or mixed ILs in a 30-ml glass vial. We expanded the treatment system in the ratio for enzymatic hydrolysis. The sample was prepared under a nitrogen atmosphere to prevent uptake of water by the ILs. After a vigorous agitation, the IL solution should turn clear. The solution was heated in an oil bath with magnetic stirring at varied temperatures from 80 to 130 $^{\circ}\text{C}$, dissolved and incubated for 20 min. Cellulose was also treated at 60 $^{\circ}\text{C}$ by deionized water for 20 min to eliminate potential difference. Deionized water was used as anti-solvent for regenerating cellulose from IL. Equal volume of water was added to the solution (Li et al. 2009). A precipitate immediately formed. The sample was briefly centrifuged. The precipitate was washed two times with additions of anti-solvent and supernatant was removed after centrifugation, and the treated cellulose was air-dried.

Enzymatic hydrolysis

Batch enzymatic hydrolysis of IL-treated and water-treated cellulose was carried out at 50 $^{\circ}\text{C}$ in a water bath shaker. Total batch volume was 50 ml with an enzyme concentration of 90 FPU per gram of cellulose and substrate concentration of about 18 mg/ml. Solutions were buffered with 0.05 M sodium citrate, pH 5.0. The enzyme reaction was monitored by withdrawing samples from the supernatant using a micro-sampler periodically and measuring the release of soluble reducing sugars by the DNS assay (Miller 1959) and glucose

by Biosensor analyzer SBA40D, Shandong Academy of Sciences Co., Ltd. Control assays (applying denatured enzyme) were made in parallel to the enzymatic ones. Subsequently, the fibers were washed three times with water and recovered by filtration for monitoring the deviation of DP with enzymatic hydrolysis. Each time, the filtrate was forced to pass through the fiber cake in order to avoid the loss of the shorter fibers. DP value of recovered cellulose was determined by the Nelson–Somogyi method (Nelson 1944). All assays were run in triplicate. Error bars indicate the standard deviation of triplicate measurements.

Analytical methods

The viscosity of ionic liquid and cellulose/IL solution was determined using HAAKE Rheostress 600 equipped with an oil bath (Brookfield Engineering Laboratories, Inc.). Viscosity of ionic liquid ([EMIM][Cl], [BMIM][Cl], [EMIM][HSO₄], [BMIM][HSO₄], [DMIM][DMP] and [EMIM][DEP]) and mixed ionic liquids ([EMIM][Cl] + [EMIM][HSO₄], [BMIM][Cl] + [EMIM][HSO₄], [DMIM][DMP] + [EMIM][HSO₄] and [EMIM][DEP] + [EMIM][HSO₄]) was measured from 50 to 130 °C. Viscosity of cellulose/IL solution in the ratio of 3/100 (wt) was measured from 80 to 130 °C. Degree of polymerization was calculated according to the viscosimetric method. This method is based on the measurement of the flowing time of a cellulose solution (using cupriethylenediamine as solvent) in a capillary viscosimeter at 25 °C. The intrinsic viscosity, $[\eta]$, of each solution is determined according to the Martin equation. DP values are calculated by applying the Immergut formula: $DP^{0.905} = 0.805 \cdot [\eta]$ (Pala et al. 2007). All experiments were run in triplicate.

Cellulose treated with water at 60 °C and cellulose treated with IL ([EMIM]Cl, [BMIM]Cl, [DMIM][DMP], [EMIM][DEP], [BMIM][HSO₄], [EMIM][HSO₄], [EMIM]Cl + [EMIM][HSO₄], [BMIM]Cl + [EMIM][HSO₄], [DMIM][DMP] + [EMIM][HSO₄] and [EMIM][DEP] + [EMIM][HSO₄]) were analyzed by FT-IR through the following process: cellulose was measured by Bruker IR spectrometer Tensor 27. The spectra (4000–400 cm⁻¹) were recorded with a resolution of 4 cm⁻¹ and 64 scans per sample. About 2.0 mg samples were prepared by mixing with 120.0 mg of spectroscopic grade KBr and then pressed with a standard device using a pressure of 6000 psi to produce 13-mm-diameter pellets (Feng et al. 2014). The background spectrum of pure KBr was subtracted from that of the sample spectrum.

Scanning electron microscopy (SEM) was carried out to obtain images of cellulose samples which were treated with water at 60 °C, [DMIM][DMP] and [DMIM][DMP] + [EMIM][HSO₄] at 130 °C. The samples were coated with a thin gold layer using a vacuum sputter coater

to improve the conductivity of the samples and thus the quality of the SEM images prior to the analysis. Scanning electron microscopy (HITACHI S-3400) operated at 5 keV was used to image cellulose samples.

Cellulose treated with water at 60 °C and [DMIM][DMP], [DMIM][DMP] + [EMIM][HSO₄] at 130 °C were analyzed using Thermogravimetric analysis (TGA). It was carried out with PerkinElmer Pyris TGA instrument under a nitrogen atmosphere (50 mL min⁻¹). To minimize possible differences in the moisture content between samples, all samples were equilibrated at 110 °C for 5 min before heating. The temperature was raised from 25 to 600 °C at a heating rate of 10 °C min⁻¹. The decomposition temperature T_{dcp} represents the thermal onset of decomposition, signifying the occurrence of a 10% total mass loss during TGA scanning at 10 °C min⁻¹.

Water-treated, IL-treated and mixed ILs-treated cellulose were analyzed by X-ray powder diffraction (XRD). XRD was conducted with an X'PERT PRO powder diffractometer PANalytical with X'celerator detector using Nickel filtered CuK α radiation at 40 kV and 30 mA was used. Samples were scanned by XRD over the angular range 5.0°–60°, 2θ , with continuous scan.

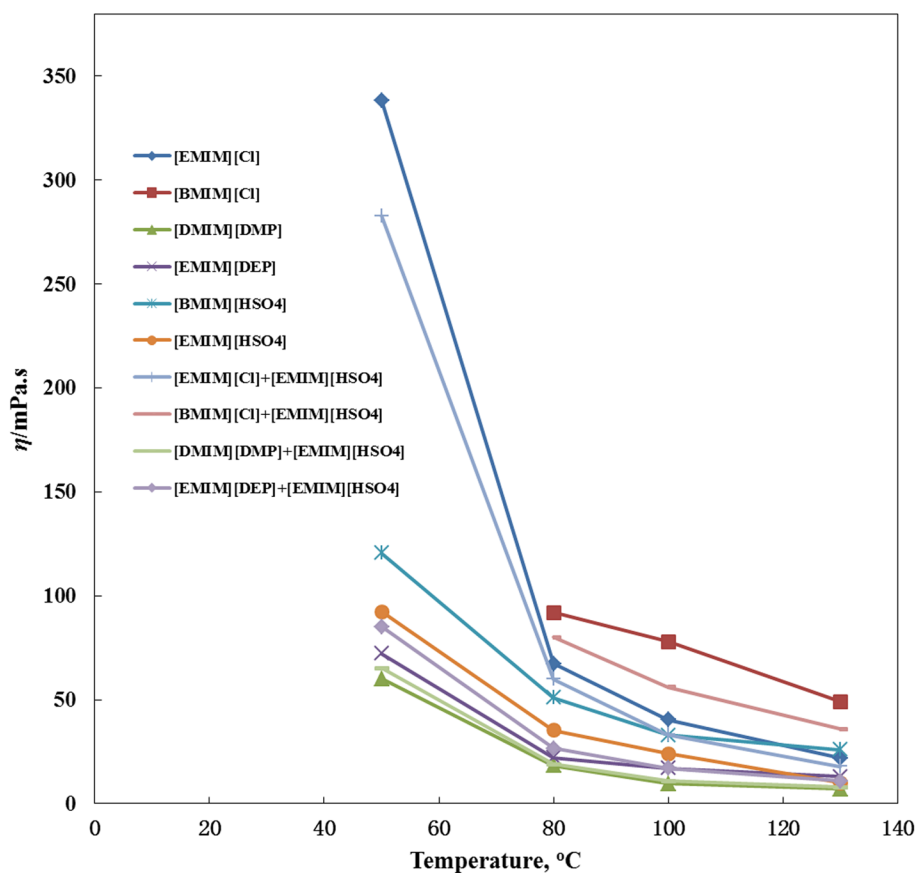
Results and discussion

Viscosity of ionic liquid and cellulose/ionic liquid solution

In order to better understand polymer behavior related to enzymatic conversion in a cellulose/ionic liquid solution, we evaluated the properties of each IL and cellulose/ionic liquid solution for interactions between solvent components which are of great importance for the understanding of cellulose phase diagram.

In our case, IL or mixed ILs and dissolved at 50–130 °C. The ILs are viscous at 50 °C (higher than 60 mPa s), and the viscosity decreased sharply with the increase in temperature from 50 to 130 °C (Fig. 1). If the viscosity of an ionic liquid is very high, it will be detrimental to the progress of a reaction. Chloride-type IL was observed to be the highest viscosity at all temperatures, followed by phosphate-type ILs and bisulfate-type IL. As shown in Fig. 1, the viscosity of phosphate-type ILs at 80 °C was 18.3 mPa s and 22.1 mPa s for IL [DMIM][DMP] and [EMIM][DEP], indicating that viscosity of IL decreased with the decrease in molecular weight. A similar trend was observed in mixed ILs samples. The addition of IL with low viscosity strongly decreases the viscosity of chloride-type IL, as expected. [EMIM][HSO₄] was selected as a candidate for the subsequent process because it is less viscous than [BMIM][HSO₄] (Fig. 1). In contrast, no obvious deviation of characteristics was

Fig. 1 Viscosity of ionic liquid and mixed ionic liquids. The intrinsic viscosity, $[\eta]$, of each solution is determined according to the Martin equation. DP values are calculated by applying the Immergut formula: $DP^{0.905} = 0.805 \cdot [\eta]$ (Pala et al. 2007)



observed when we mixed phosphate-type IL with chloride-type IL (data not shown). Consequently, mixed ILs solution was prepared by mixing cellulose dissolving [DMIM][DMP] with bisulfate-type ionic liquid ([EMIM][HSO₄]) to develop new and multifold function. Viscosity of [EMIM]Cl + [EMIM][HSO₄] mixture (a kind of mixed ionic liquids) was sharply reduced when we mixed 0.9 g [EMIM]Cl with 0.1 g [EMIM][HSO₄] (9:1 in the ratio). The proportion of [DMIM][DMP] and [EMIM][HSO₄] could also be confirmed by enzymatic hydrolysis of cellulose treated with mixed ionic liquids (Fig. S1). Therefore, cellulose dissolving IL and [EMIM][HSO₄] in the ratio of 9:1 was used in the subsequent process.

Cellulose was added to IL or mixed ILs and dissolved at 80–130 °C. Practically speaking, detection of cellulose/IL solutions in high concentrations and low temperatures is difficult to reach because of very high viscosity and thus very slow dissolution kinetics. So, the viscosity of 3% (w/w%) cellulose in phosphate-type IL or phosphate-type IL mixed with bisulfate-type IL was determined in the range of 80–130 °C (Fig. 2). The intrinsic viscosity measurement is a fast and convenient method to estimate the average DP of cellulose and thus the extent of degradation (Michud et al. 2015). Moreover, the determination of DP provides only some information on the viscosity-average molar

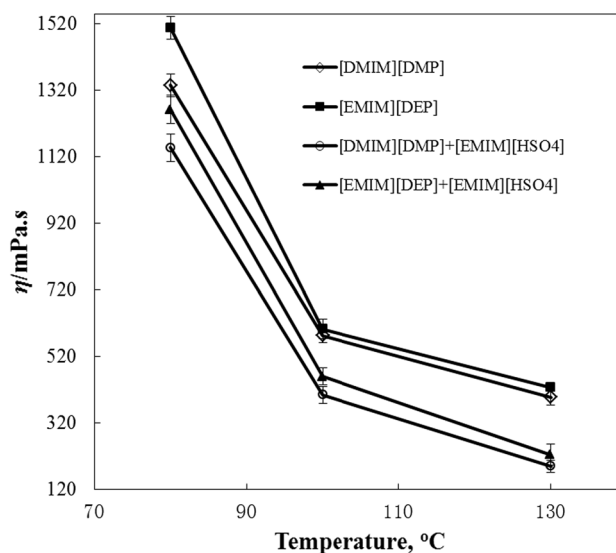


Fig. 2 Viscosity of cellulose/IL solution. The intrinsic viscosity, $[\eta]$, of each solution is determined according to the Martin equation. DP values are calculated by applying the Immergut formula: $DP^{0.905} = 0.805 \cdot [\eta]$ (Pala et al. 2007)

mass and no element regarding the molar mass distribution (Michud et al. 2015). Cellulose/mixed ILs showed a lower

viscosity than that of cellulose/single IL, while viscosity of the solution decreased with the decrease in molecular weight. For an example, viscosity decline of cellulose/([DMIM][DMP] + [EMIM][HSO₄]) is pronounced from 1147 to 190 mPa s when the treatment temperature increased from 80 to 130 °C (Fig. 2), implying that the drop of viscosity to lower values demonstrated a liquid-like behavior. The deviation of experimental results indicated that mixed ionic liquids reduced the viscosity of the solution, which will subsequently influence cellulose solubility and following enzymatic conversion of cellulose.

FT-IR, XRD and SEM images analysis of IL- or mixed ILs-treated cellulose

To visualize the variation of cellulose structure treated by IL, we compared the infrared spectra XRD and SEM images of water-treated cellulose and ionic liquid-treated cellulose. From spectra of FT-IR, two infrared ratios were calculated: (1) $\alpha_{1437\text{ cm}^{-1}}/\alpha_{899\text{ cm}^{-1}}$, which is referred as the crystallinity index (O'Connor et al. 1958) or lateral order index (LOI) (Hurtubise and Krassig 1960), (2) $\alpha_{1378\text{ cm}^{-1}}/\alpha_{2900\text{ cm}^{-1}}$, which is known as the total crystallinity index (TCI) (Nelson and O'Connor 1964a, b). The higher index value represents the material has a higher crystallinity and ordered structure (Li et al. 2009). As shown in Table 1, after dissolved and incubated in phosphate-type IL or chloride-type ionic liquid at 130 °C for 20 min, the LOI and TCI of cellulose decreased after single IL treatment and mixed ILs treatment compared with water-treated cellulose (LOI = 1.34, TCI = 1.22). IL can effectively convert cellulose I structure to cellulose II, decreasing the crystallinity of cellulose and increasing the structural homogeneity (Li et al. 2010), while there was almost no difference in LOI and TCI between [EMIM][HSO₄]-treated cellulose and water-treated cellulose (control), indicating IL [EMIM][HSO₄] pose almost no effect on the structure of cellulose for the IL could not dissolve

cellulose. Interestingly, LOI and TCI of cellulose were significantly decreased when treated by mixed IL ([EMIM][HSO₄] mixed with cellulose dissolving ionic liquids). The lowest value of LOI (0.73) and TCI (0.39) was obtained from cellulose treated by mixture of [DMIM][DMP] and [EMIM][HSO₄] at 130 °C for 20 min (Table 1), suggesting that cellulose treated by mixed IL is less crystalline compared to single phosphate-type IL- or water-treated samples. Therefore, [DMIM][DMP] and [EMIM][HSO₄] were selected in the subsequent process.

The XRD patterns of cellulose pretreated with [EMIM][HSO₄], [DMIM][DMP] and [DMIM][DMP] + [EMIM][HSO₄] indicated in Fig.S2.b, Fig.S2.c and Fig.S2.d as diffractograms, respectively, mirror the diffractograms detected for water-treated sample (Fig.S2.a). [EMIM][HSO₄] do not induce obvious changes in the pretreated cellulose (Fig.S2.b and Fig.S2.d), which is similar to the work of Bernardo et al. (Bernardo et al. 2019). It is demonstrated in Figure S2.c and S2.d that the noticeable transformation is a disappearance of signal at 22.6° and the presence of a broad signal from 20° to 21.6°. Similarly, the broad signal from 14.6° to 16.0° disappeared and was substituted with a new signal emerged at 12.1° (Fig.S2.c and Fig.S2.d). It is indicated that transformation of cellulose I to cellulose II (Bernardo et al. 2019), resulting in better enzymatic hydrolysis.

SEM images of water-treated and IL-treated cellulose are displayed in Fig. 3. Long fibers (Fig. 3a1) of cellulose treated by water (control) showed a highly ordered organization of well-separated fibers (Raut et al. 2015). Compared with water-treated cellulose (Fig. 3a1, a2, a3), more rupture and porous fibers and more free of trenches were observed in cellulose treated by [DMIM][DMP] (single IL) (Fig. 3b). Surface of cellulose granule became rough and swollen (Fig. 3b2, b3) form after [DMIM][DMP] treatment which was also reported on cellulosic biomass treated with phosphate-type IL (Yang et al. 2010). Particularly, around 3–6 μm cellulose particles were obtained after mixed ILs

Table 1 Infrared ratio and polymerization degree of cellulose samples

Treatment reagent	LOI (1437/899 cm ⁻¹)	TCI (1378/2900 cm ⁻¹)	DP value
[EMIM]Cl	1.19	1.00	330
[BMIM]Cl	1.20	1.12	350
[DMIM][DMP]	0.94	0.86	280
[EMIM][DEP]	1.04	1.00	300
[BMIM][HSO ₄]	1.31	1.22	661
[EMIM][HSO ₄]	1.30	1.22	663
[EMIM]Cl + [EMIM][HSO ₄]	0.98	0.62	254
[BMIM]Cl + [EMIM][HSO ₄]	1.10	0.96	260
[DMIM][DMP] + [EMIM][HSO ₄]	0.73	0.39	208
[EMIM][DEP] + [EMIM][HSO ₄]	0.88	0.52	210
Water	1.34	1.22	676

Cellulose dissolving ionic liquids: [EMIM]Cl, [BMIM]Cl, [DMIM][DMP], [EMIM][DEP]

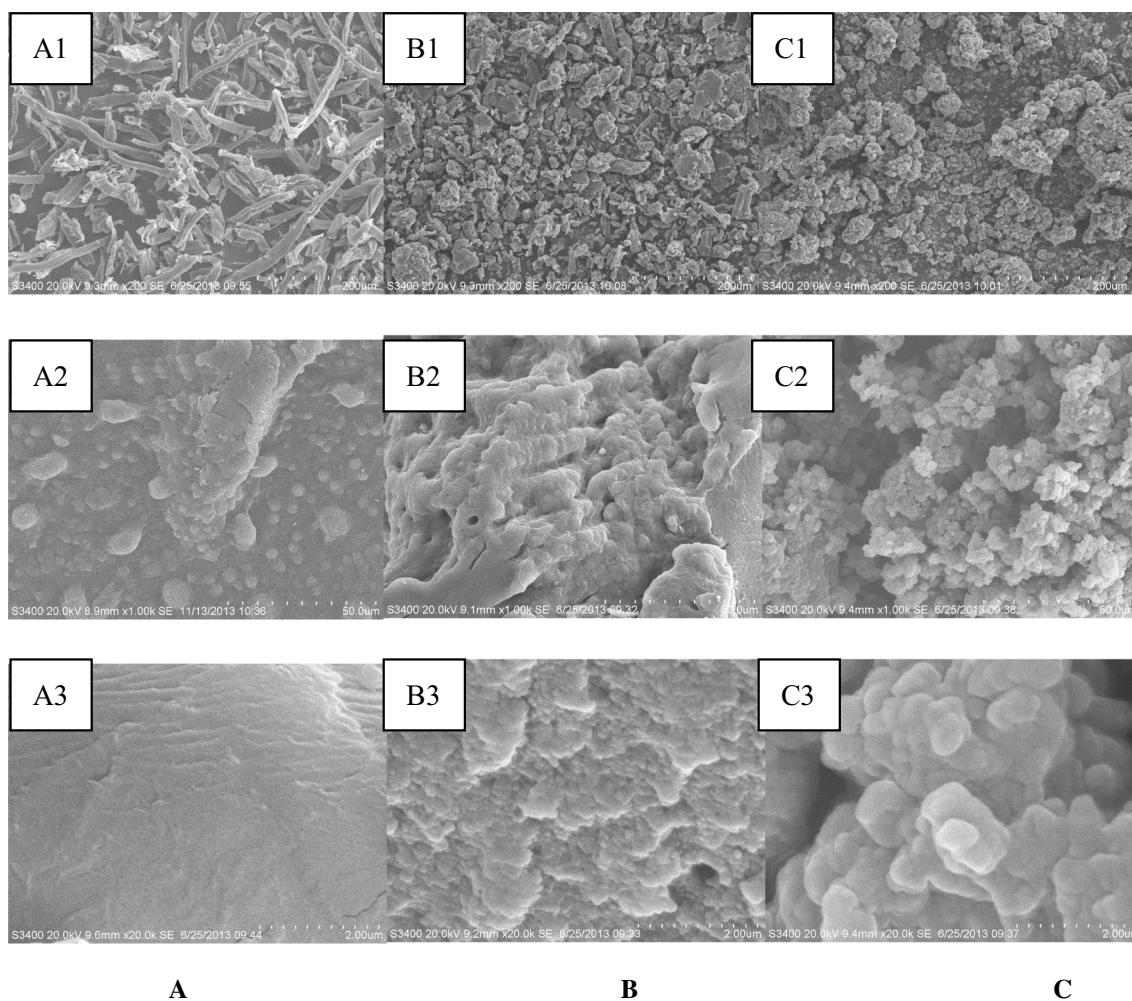


Fig. 3 SEM image of water-treated cellulose and ionic liquid-treated cellulose. **a** Water-treated cellulose. **b** [DMIM][DMP] ionic liquid-treated cellulose. **c** [DMIM][DMP] and [EMIM][HSO₄]-treated cellulose

([DMIM][DMP] + [EMIM][HSO₄]) treatment (Fig. 3c). The organization of macrofibrils was completely destroyed, and particles were agglomerated like nanomaterials (Fig. 3c2, c3) which is first reported, implying that the structural transformation generated by the mixed ILs treatment had led to enhanced accessible possibility and larger surface responsible (De Melo et al. 2017) for the highest increase in cellulose degradation (Fig. 3 and Table 1). So, the phosphate-type ILs and IL [EMIM][HSO₄] were selected as candidate solvents for the subsequent treatment of cellulose.

Thermogravimetric scans comparison of cellulose samples

The thermal stability of cellulose from water treatment and ionic liquid treatment was determined by TGA analysis. The curves show similar trends with weight losses starting at 25 °C and reaching quasi-plateau regions, before

the final degradation of the material. As shown in Fig. 4, water-treated cellulose gave the highest T_{dcp} value of 316 °C, followed by cellulose treated with ionic liquid [DMIM][DMP] (244 °C), and finally cellulose treated by [DMIM][DMP] + [EMIM][HSO₄] (216 °C). Similar trend was also observed by Tang et al. (Tang et al. 2012). Understandably, the least thermally stable cellulose is the one that is most severely modified in terms of the crystallinity index and overall morphology, as also confirmed by SEM and XRD analysis. Thus, variation in the thermal stability of cellulose serves as an indirect indicator of the degree of structural modification ensuing from mixed ILs treatment.

Enzymatic hydrolysis of cellulose samples

It is expected that the DP value provided varies according to the method used and to the complexity of the material. Therefore, it has been of interest for several authors to

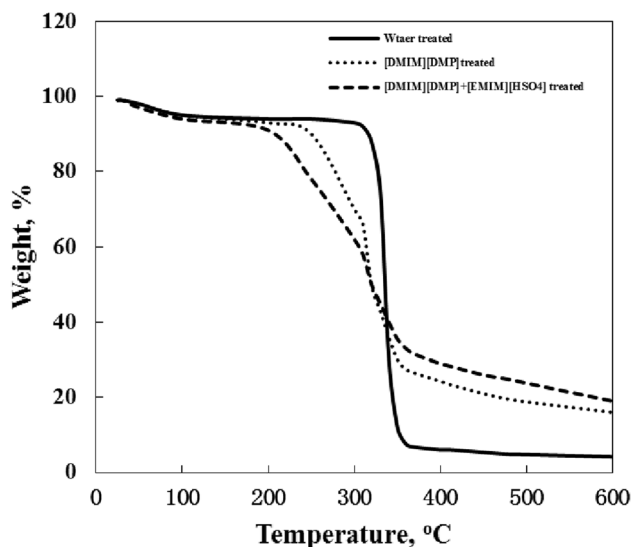


Fig. 4 Thermogravimetric scans comparing the thermal stability of water-treated cellulose with cellulose pretreated with ionic liquid [DMIM][DMP] and [DMIM][DMP] + [EMIM][HSO₄]

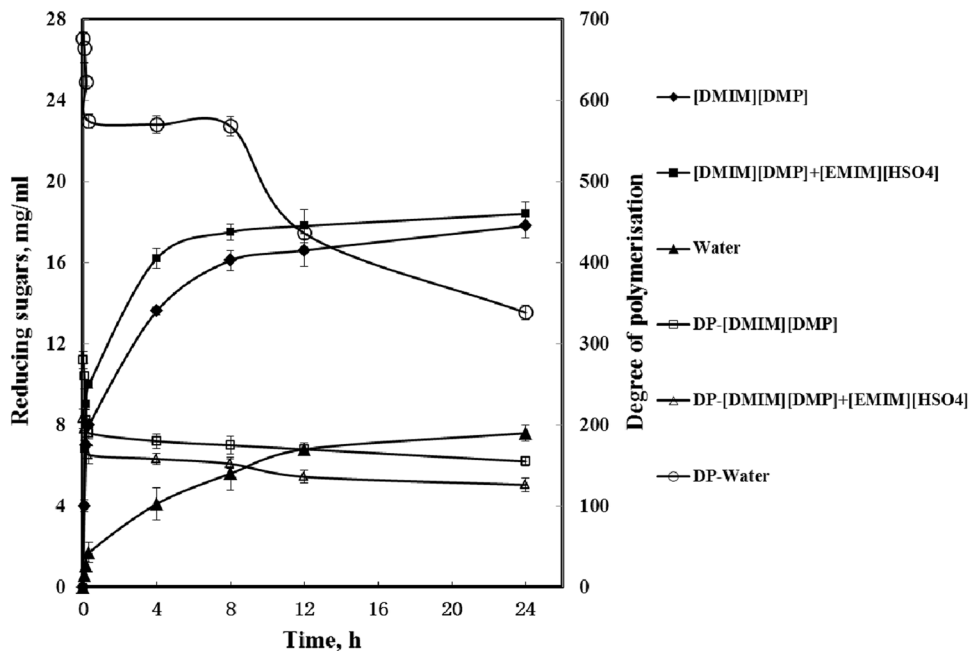
discuss the DP values obtained by using different methods. Pala et al. (2007) analyzed DP value deviation of paper pulps and commercial powder cellulose before and after the enzymatic hydrolysis and established enzymes mode of action on the fibers. Compared with water-treated sample, DPs of cellulose were decreased when treated with single IL and mixed ILs. Cellulose macromolecule was destroyed when treated by IL. Cellulose was fragmented by mixed ILs treatment and DPs decreased from 676 to 254, 260, 208 and 210 after treated by IL mixture of [EMIM]Cl + [EMIM][HSO₄],

[BMIM]Cl + [EMIM][HSO₄], [DMIM][DMP] + [EMIM][HSO₄], [EMIM][DEP] + [EMIM][HSO₄] (Fig. 5), respectively. Likewise, similar results were observed using morpholinium IL as solvent (single IL) (Raut et al. 2015). It is recognized that the longer molecules have a corresponding larger weight on these DP values (Table 1), which is agreed with the results of the SEM image (Fig. 3). The longer and more flexible molecules have an effect on viscosity (Fig. 1) that is more than proportional to the molecular weight (Pala et al. 2007); as the solvent occupies a large part of the effective hydrodynamic sphere of the larger molecules, the smaller molecules have the lower contribution to the viscosity of the cellulose/IL solution (Fig. 2). In our case, [DMIM][DMP] + [EMIM][HSO₄] was confirmed to be good reagent for treatment of cellulose, resulting cellulose sample with low DP value 208 (Table 1).

The same general trend on the DP variation is observed with enzymatic hydrolysis irrespective of the measuring technique: a sharp decrease in DP values is detected in all enzymatic hydrolyzed samples (Fig. 5). The significant DP variation occurs within 20 min, which is in accordance with the higher solubilization at that time; after that period, the DP variation is less important and suggests the decrease in the endoglucanase activity (Van Wyk 1997). In water-treated cellulose, the low surface area limits the endoglucanase accessibility and possibility (according to SEM image analysis, Fig. 3) to β -glucosidase bonds and hence the decrease in DP is not as rapid as in the IL-treated cellulose and the native cellulose remains insoluble.

There are many compositions in cellulosic biomass such as cellulose, lignin, hemicellulose, wax, pectin, protein and others (Ten and Vermerris 2013) which will affect analysis

Fig. 5 Enzymatic hydrolysis of cellulose samples with a variety of their DP. Cellulose samples were incubated in phosphate-type IL or chloride-type ionic liquid at 130 °C for 20 min. Conversion of cellulose to sugars for batch samples of 18 mg/ml cellulose hydrolyzed with 90 FPU *Aspergillus niger* cellulase per gram cellulose at 50 °C is shown as a function of time for total soluble sugars (measured using a DNS assay)



of DP, TGA, CrI, XRD and enzymatic hydrolysis. Cellulose is isolated from natural biomass and milled into 50 μm particles to obtain cellulose PH101. There are no influence factors in it. Therefore, we used cellulose PH101 as substrate to evaluate the effect of cellulose pretreatment with ionic liquid or mixed ionic liquids. The dissolved cellulose was further precipitated by the addition of deionized water (Dadi et al. 2006). Clearly, the conversion of treated cellulose to reducing sugar appeared to be higher than that of water-treated one (control) (Fig. 5). Using IL as treatment solvent, the conversions of treated cellulose to reducing sugars appeared to at least two folds than that of water-treated one. The significant hydrolysis of cellulose was observed in the beginning of the reaction (20 min). Both the hydrolysis rates and sugars formation rates were significantly greater for the IL-treated cellulose samples compared to those for water-treated cellulose (Fig. 5).

Batch enzymatic hydrolysis of IL-treated and water-treated cellulose was carried out at 50 $^{\circ}\text{C}$ in a water bath shaker. Control assays (applying denatured enzyme) were made in parallel to the enzymatic ones. Initial rate of releasing of total soluble reducing sugars were measured by DNS assay in enzymatic hydrolysis of cellulose. Cellulose samples were dissolved and incubated for 20 min at 130 $^{\circ}\text{C}$ and precipitated using the water. Rates are calculated from data obtained in the first 20 min of enzymatic hydrolysis. The initial rates of enzymatic hydrolysis of cellulose treated by water (control), [DMIM][DMP] and mixed IL ([DMIM][DMP] + [EMIM][H₂SO₄]) were 0.0140, 0.7368 and 0.7882 $\text{mg/ml}^{-1} \text{min}^{-1}$. Rate enhancement of enzymatic hydrolysis is defined as the ratio of initial rate of reducing sugars released for treated cellulose divided by that of water-treated cellulose. Rate enhancement of enzymatic hydrolysis of IL [DMIM][DMP] and mixed ILs ([DMIM][DMP] + [EMIM][H₂SO₄]) in the ratio of 9:1 was 52.6 (similar to the result of Dadi et al. 2006) and 56.3 times that of water-treated cellulose. Both the hydrolysis rates and rates of sugars formation were significantly greater for the treated cellulose samples compared to those for water-treated cellulose (Fig. 5). The amount of reducing sugars released from [DMIM][DEP]-treated, [DMIM][DMP] + [EMIM][H₂SO₄]-treated cellulose and water-treated cellulose during the first 4 h of enzymatic hydrolysis reaction was 13.6, 16.2 and 4.1 mg/ml (Fig. 5), implying that enzymatic conversion rate of cellulose to reducing sugars was 2.32 and 2.95 times higher than that of water-treated cellulose in the first 4 h indicating amorphous structure allowing a greater number of sites (Saqib and John Whitney 2006) and more possibility for enzyme adsorption. After being enzymatically hydrolyzed for 12 h, the reducing sugars were achieved in the concentrations of 16.6, 17.8 and 6.8 mg/ml using single IL ([DMIM][DEP]), mixed ILs ([DMIM][DMP] + [EMIM][H₂SO₄]) and water treatment, respectively, while enzymatic

hydrolysis rates and rates of glucose formation were obviously greater for the IL-treated cellulose samples compared to those for water-treated one. The releasing glucose of [DMIM][DMP] + [EMIM][H₂SO₄]-treated sample is much faster than [DMIM][DMP]-treated one. For example, after 8 h 9.3 mg/ml and 11.5 mg/ml glucose were obtained compared to only 4.0 mg/ml glucose was obtained from the water-treated cellulose (Fig. S3.).

Conclusions

In our approach, mixed ionic liquids were developed to treat cellulose for efficient cellulase enzymatic conversion. FT-IR, SEM, XRD, TGA and DP were used to measure the alteration of structure and intrinsic characters in cellulose, resulting in amorphous structure allowing a greater number of sites and more possibility for enzyme adsorption with subsequent enhancement of hydrolysis kinetics. Almost all cellulose was hydrolyzed within 12 h of enzymatic hydrolysis for mixed ILs-treated sample. Unlike some other studies, not only outermost surface of cellulose was changed, but the intact structure of cellulose was destroyed and converted into micron-sized particles. The results are also attractive to application in other enzymatic conversions.

Acknowledgements The authors would like to acknowledge the research grant provided by the Postdoctoral Science Foundation of China (2013M541644), Postdoctoral Science Foundation of Jiangsu Province (1302128C) and Jiangsu Overseas Research & Training Program for University Prominent Young & Middle-aged Teachers and Presidents.

Compliance with ethical standards

Conflict of interest We declare that we have no financial and personal relationships with other people or organizations that can inappropriately influence our work, and there is no professional or other personal interest of any nature or kind in any product, service and/or company that could be construed as influencing the position presented in, or the review of, the manuscript entitled "Efficient enzymatic hydrolysis of cellulose treated by mixed ionic liquids."

References

- Bernardo JR, Gírio FM, Łukasik RM (2019) The effect of the chemical character of ionic liquids on biomass pre-treatment and posterior enzymatic hydrolysis. *Molecules* 24:1–17. <https://doi.org/10.3390/molecules24040808>
- Chen YW, Lee HV (2020) Recent progress in homogeneous Lewis acid catalysts for the transformation of hemicellulose and cellulose into valuable chemicals, fuels, and nanocellulose. *Rev Chem Eng* 36(2):215–235. <https://doi.org/10.1515/revce-2017-0071>
- Dadi AP, Varanasi S, Schall CA (2006) Enhancement of cellulose saccharification kinetics using an ionic liquid pretreatment step. *Biotechnol Bioeng* 95:904–910. <https://doi.org/10.1002/bit.21047>

- De Melo RP, Marques MF, Navard P, Duque NP (2017) Degradation studies and mechanical properties of treated curauá fibers and microcrystalline cellulose in composites with polyamide 6. *J Compos Mater* 51(25):3481–3489. <https://doi.org/10.1177/0021998317690446>
- Feng YY, Li Q, Kang G, Ji G, Tang Y, Tu J (2014) Aqueous two-phase/reverse micelle continuous process for recycling and simultaneous purification of polar ionic liquid from enzymatic hydrolysate. *J Chem Technol Biot* 91(2):394–399. <https://doi.org/10.1002/jctb.4587>
- Haldar D, Purkait MK (2020) Lignocellulosic conversion into value-added products: a review. *Process Biochem* 89:110–133. <https://doi.org/10.1016/j.procbio.2019.10.001>
- Houfani AA, Anders N, Spiess AC, Baldrian P, Benallaoua S (2020) Insights from enzymatic degradation of cellulose and hemicellulose to fermentable sugars—a review. *Biomass Bioenergy* 134:105481. <https://doi.org/10.1016/j.biombioe.2020.105481>
- Huang X, Yamasaki K, Kudo S, Sperry J, Hayashi J (2020) Influence of ionic liquid type on porous carbon formation during the ionothermal pyrolysis of cellulose. *J Anal Appl Pyrol* 145:104728. <https://doi.org/10.1016/j.jaap.2019.104728>
- Hurtubise FG, Krassig H (1960) Classification of fine structural characteristics in cellulose by Infrared Spectroscopy. Use of potassium bromide pellet technique. *Anal Chem* 32:177–181. <https://doi.org/10.1021/ac60158a010>
- Jang SK, Lee JH, Jung CD, Yu JH, Choi JW, Choi IG, Kim H (2020) High yield solvent extraction of hydrothermal and ball-milling treated lignin prior to enzymatic hydrolysis for co-valorization of lignin and cellulose in *Miscanthus sacchariflorus*. *Fuel* 269:117428. <https://doi.org/10.1016/j.fuel.2020.117428>
- Jiang LQ, Liu QL, Lin Y, Xu FX, Zhang X, Zhao ZL, Li HB (2020) Impact of ball-milling and ionic liquid pretreatments on pyrolysis kinetics and behaviors of crystalline cellulose. *Bioresour Technol* 305:123044. <https://doi.org/10.1016/j.biortech.2020.123044>
- Kim S, Seo AY, Lee TG (2020) Functionalized cellulose to remove surfactants from cosmetic products in wastewater. *Carbohydr Polym* 236:116010. <https://doi.org/10.1016/j.carbpol.2020.116010>
- Li Q, He YC, Xian M, Jun G, Xu X, Yang JM, Li LZ (2009) Improving enzymatic hydrolysis of wheat straw using ionic liquid 1-ethyl-3-methylimidazolium diethyl phosphate pretreatment. *Bioresour Technol* 100(14):3570–3575. <https://doi.org/10.1016/j.biortech.2009.02.040>
- Li Q, Jiang X, He Y, Li LZ, Xian M, Yang J (2010) Evaluation of the biocompatible ionic liquid 1-methyl-3-methylimidazolium dimethylphosphate pretreatment of corn cob for improved saccharification. *Appl Microbiol Biotechnol* 87:117–126. <https://doi.org/10.1007/s00253-010-2484-8>
- Li DQ, Jinfeng W, Xi L, Wu C, Xiongwei D, Bin T, Xungai W (2019) One-step firing of cellulose fiber and ceramic precursors for functional electro-thermal composites. *Mater Des* 181:107941–107949. <https://doi.org/10.1016/j.matdes.2019.107941>
- Liu ZH, Li Longfei, Liu Cheng, Airon Xu (2017) Saccharification of cellulose in the ionic liquids and glucose recovery. *Renew Energy* 106:99–102. <https://doi.org/10.1016/j.renene.2017.06.040>
- Lv W, Liao YH, Zhu YT, Liu J, Zhu CH, Wang CG, Xu Y, Zhang Q, Chen GY, Ma LL (2020) The effect of Ru/C and MgCl₂ on the cleavage of inter- and intra-molecular linkages during cornstarch hydrolysis residue valorization. *Cellulose* 27(2):799–823. <https://doi.org/10.1007/s10570-019-02799-x>
- Michud A, Hummel M, Haward S, Sixta H (2015) Monitoring of cellulose depolymerization in 1-ethyl-3-methylimidazolium acetate by shear and elongational rheology. *Carbohydr Polym* 117:355–363. <https://doi.org/10.1016/j.carbpol.2014.09.075>
- Miller GL (1959) Use of dinitrosalicylic acid reagent for determination of reducing sugar. *Anal Chem* 31:426–428. <https://doi.org/10.1021/ac60147a030>
- Nelson N (1944) A photometric adaptation of the Somogyi method for the determination of glucose. *J Biol Chem* 153:375–380. <https://doi.org/10.1017/S0009840X00101660>
- Nelson ML, O'Connor RT (1964a) Relation of certain infrared bands to cellulose crystallinity and crystal lattice type. Part II. A new infrared ratio for estimation of crystallinity in celluloses I and II. *J Appl Polym Sci* 8:1325–1341. <https://doi.org/10.1002/app.1964.070080323>
- Nelson ML, O'Connor RT (1964b) Relation of certain infrared bands to cellulose crystallinity and crystal lattice type. Part I. Spectra of lattice types I, II, III and of amorphous cellulose. *J Appl Polym Sci* 8:1311–1324. <https://doi.org/10.1002/app.1964.070080323>
- Nie Y, Li C, Sun A, Meng H, Wang Z (2006) Extractive desulfurization of gasoline using imidazolium-based phosphoric ionic liquids. *Energy Fuels* 20:2083–2087. <https://doi.org/10.1021/ef060170i>
- O'Connor RT, DuPré EF, Mitcham D (1958) Applications of Infrared Absorption Spectroscopy to investigations of cotton and modified cottons: part I: physical and crystalline modifications and oxidation. *Text Res J* 28:382–392. <https://doi.org/10.1177/004051755802800702>
- Pala H, Mota M, Gama FM (2007) Enzymatic depolymerisation of cellulose. *Carbohydr Polym* 68:101–108. <https://doi.org/10.1016/j.carbpol.2006.07.015>
- Ratnasari DK, Horn A, Brunner T, Yang WH, Jonsson PG (2019) The thermal degradation of lignocellulose biomass with an acid leaching pre-treatment using a H-ZSM-5/Al-MCM-41 catalyst mixture. *Fuel* 257:1160861–1160868. <https://doi.org/10.1016/j.fuel.2019.116086>
- Raut DG, Sundman O, Su W, Virtanen P, Sugano Y, Kordas K, Mikola JP (2015) A morpholinium ionic liquid for cellulose dissolution. *Carbohydr Polym* 130:18–25. <https://doi.org/10.1016/j.carbpol.2015.04.032>
- Saqib AAN, John Whitney P (2006) Role of fragmentation activity in cellulose hydrolysis. *Int Biodeterior Biodegrad* 58:180–185. <https://doi.org/10.1016/j.ibiod.2006.06.007>
- Shah TA, Ullah R (2019) Pretreatment of wheat straw with ligninolytic fungi for increased biogas productivity. *Int J Environ Sci Technol* 16(11):7497–7508. <https://doi.org/10.1007/s13762-019-02277-8>
- Sievers DA, Kuhn EM, Tucker MP, McMillan JD (2017) Effects of dilute-acid pretreatment conditions on filtration performance of corn stover hydrolyzate. *Bioresour Technol* 243:474–480. <https://doi.org/10.1016/j.biortech.2017.06.144>
- Sirvio JA, Hyypio K, Asaadi S, Junka K, Liimatainen H (2020) High-strength cellulose nanofibers produced via swelling pretreatment based on a choline chloride-imidazole deep eutectic solvent. *Green Chem* 22(5):1763–1775. <https://doi.org/10.1039/c9gc04119b>
- Tan XY, Chen L, Li XX, Xie FW (2019) Effect of anti-solvents on the characteristics of regenerated cellulose from 1-ethyl-3-methylimidazolium acetate ionic liquid. *Int J Biol Macromol* 124:314–320. <https://doi.org/10.1016/j.ijbiomac.2018.11.138>
- Tang S, Baker GA, Ravula S, Jones JE, Zhao H (2012) PEG-functionalized ionic liquids for cellulose dissolution and saccharification. *Green Chem* 14:2922–2932. <https://doi.org/10.1039/C2GC35631G>
- Ten E, Vermerris W (2013) Functionalized polymers from lignocellulosic biomass: state of the art. *Polymers* 5:600–642. <https://doi.org/10.3390/polym5020600>
- Ullah H, Hélder AS, Khan T (2016) Applications of bacterial cellulose in food, cosmetics and drug delivery. *Cellulose* 23(4):2291–2314. <https://doi.org/10.1007/s10570-016-0986-y>
- Van Wyk JPH (1997) Cellulase adsorption-desorption and cellulose saccharification during enzymatic hydrolysis of cellulose materials. *Biotechnol Lett* 19:775–778. <https://doi.org/10.1023/a:1018392326999>

- Xu JK, Dai L, Zhang CT, Gui Y, Yuan L, Lei Y, Fan BA (2020) Ionic liquid-aided hydrothermal treatment of lignocellulose for the synergistic outputs of carbon dots and enhanced enzymatic hydrolysis. *Bioresour Technol* 305:123043. <https://doi.org/10.1016/j.biortech.2020.123043>
- Yang F, Li L, Li Q, Tan WQ, Liu W, Xian M (2010) Enhancement of enzymatic in situ saccharification of cellulose in aqueous-ionic liquid media by ultrasonic intensification. *Carbohydr Polym* 81:311–316. <https://doi.org/10.1016/j.carbpol.2010.02.031>
- Zhu SY, Xu J, Cheng Z, Kuang YS, Wu QQ, Wang B, Gao WH, Zeng JS, Li J, Chen KF (2020) Catalytic transformation of cellulose into

short rod-like cellulose nanofibers and platform chemicals over lignin-based solid acid. *Appl Catal B Environ* 268:118732. <https://doi.org/10.1016/j.apcatb.2020.118732>

Publisher's Note Springer Nature remains neutral with regard to jurisdictional claims in published maps and institutional affiliations.